Macromolecules

ARTICLE

pubs.acs.org/Macromolecules

Bond Tension in Tethered Macromolecules

Sergei S. Sheiko,[†,*] Sergey Panyukov,[‡] and Michael Rubinstein[†]

[†]Department of Chemistry, University of North Carolina at Chapel Hill, Chapel Hill, North Carolina 27599-3290, United States

[‡]P.N. Lebedev Physics Institute, Russian Academy of Sciences, Moscow 117924, Russia

ABSTRACT: The paper presents scaling analysis of mechanical tension generated in densely branched macromolecules tethered to a solid substrate with a short linker. Steric repulsion between branches results in z-fold amplification of tension in the linker, where z is the number of chain-like arms. At large $z \sim 100-1000$, the generated tension may exceed the strength of covalent bonds and sever the linker. Two types of molecular architectures were considered: polymer stars and polymer "bottlebrushes" tethered to a solid substrate. Depending on the grafting density, one distinguishes the so-called mushroom, loose grafting, and dense grafting regimes. In isolated (mushroom) and loosely tethered bottlebrushes, the linker tension is by a factor of $\sqrt{z}$ smaller than the tension in a tethered star with the same number of arms z. In densely tethered stars, the effect of interchain distance (d) and number of arms (z) on the magnitude of linker tension is given by $f \cong f_0 z^{3/2}(b/d)$ for stars in a solvent environment and $f \cong f_0 z^2 (b/d)^2$ for dry stars, where b is the Kuhn length and $f_0 \cong k_B T/b$ is intrinsic bond tension. These relations are also valid for tethered bottlebrushes with long side chains. However, unlike molecular stars, bottlebrushes demonstrate variation of tension along the backbone $f \cong f_0 s\, z^{1/2}/d$ as a function of distance s from the free end of the backbone. In dense brushes ($d \cong b\sqrt{z}$) with $z \cong 1000$, the backbone tension increases from $f \cong f_0 \cong 1$ pN at the free end of the backbone ($s \cong b$) to its maximum $f \cong z f_0 \cong 1$ nN at the linker to the substrate ($s \cong zb$).

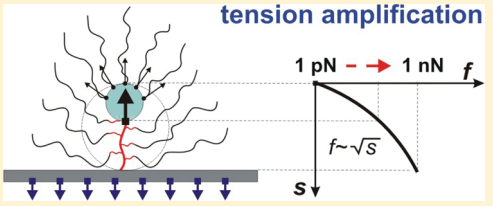

INTRODUCTION

Mechanical force is integral to all living systems[1−11] and represents one of the most common molecular stimuli, which alters electronic states evoking changes in color, conductivity, magnetism, and reactivity.[12−27] Tension in chemical bonds can be either induced or self-generated. Spontaneous, i.e. self-generated tension occurs in geometrically confined and crowded macromolecular systems, such as tethered polymer chains and polymer brushes. Already in a single polymer chain tethered to a substrate, the decrease in the number of allowed configurations leads to a noticeable tension in the first bond between the chain and substrate as[28]

$$f_0 \cong \frac{k_B T}{b} \tag{1}$$

This intrinsic tension is on the order of $f_0 \cong 1$ pN, which can be calculated from the Boltzmann's constant $k_B = 1.38 \times 10^{-23}$ J/K, an absolute temperature of $T \cong 300$ K, and a typical Kuhn length of $b \cong 1$ nm. In polymer brushes,[29−38] steric repulsion between densely grafted polymer chains causes an additional tension of $f \cong k_B T/\xi$, where ξ is the correlation length, which in a planar brush is on the order of the average distance between the neighboring grafting sites.[39,40] Since $\xi \geq b$, this tension does not exceed the tension f_0 in the linker (bond adjacent to the substrate), even for one of the highest grafting densities of $\sigma \cong 0.4$ nm^{-2} ($\xi \cong \sigma^{-1/2} \cong 1.6$ nm) reported by Fukuda et al.[41] As such, the bond tension in conventional polymer systems does not exceed several piconewtons (pN). This tension is too small to significantly alter the lifetime of covalent bonds, which exhibits an exponential force dependence

$$\tau = \tau_0 \exp\left(\frac{E_a - f b_a}{k_B T}\right) \tag{2}$$

where τ_0 is on the order of the reciprocal bond oscillation frequency, E_a is the bond activation energy, and b_a is the activation length.[42−44] For a typical covalent bond ($E_a \cong 100 k_B T$ and $b_a \cong 0.04$ nm), eq 2 gives an approximate relation for the bond lifetime as

$$\tau \cong \tau_a e^{-f/f_a} \tag{3}$$

where $\tau_a = \tau_0 \exp(E_a)/(k_B T) \cong 10^{30}$ s is a bond lifetime at a zero force and $f_a = k_B T/b_a \cong 100$ pN is a force which causes a noticeable (by a factor of e) decrease in bond lifetime. For a conventional polymer like polystyrene, this tension corresponds to a grafting density of $\sigma_a \cong 1.2$ nm^{-2}, that belong to the strongly nonlinear regime of nearly full chain extension.[45] Because of the increasingly high steric repulsion between the tethered chains, the synthesis of such dense polymer brushes is a very challenging task.

NanoNewton-level tensions in chemical bonds can be achieved through modification of a molecular architecture leading to nonuniform distribution of tension between the constituting sections. The goal is to design macromolecules that enable

Received: February 11, 2011
Revised: April 18, 2011
Published: May 10, 2011

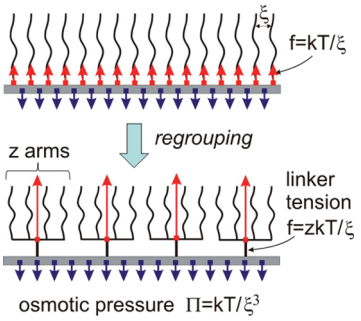

Figure 1. In polymer brushes, the osmotic pressure (downward arrows) is balanced by the tension in the linkers (upward arrows). By reconnecting the linear chains of a planar brush in groups of z arms, one gains z-fold amplification of the linker tension.

amplification, transmission, and focusing of self-generated tension at specific chemical bonds. Recently, we have demonstrated two methods of this tension management. The first method was developed for brush-like[37] and pom-pom[38] macromolecules in solution, where steric repulsion between densely packed branches builds up nanoNewton tension in the brush backbone and the pom-pom spacer, respectively. The second method was demonstrated for brush-like macromolecules physically adsorbed to an interface.[37] Adsorption significantly enhances crowdedness of the side chains causing additional amplification of tension in the brush backbone. Depending on the length of the side chains and the strength of adsorption, the backbone tension may reach values on the order of several nanoNewtons that are sufficient to instantly (seconds) sever a C−C bond (eq 3).[36,46−48]

Here we present the third method of tension amplification, which is applied to macromolecules tethered to a solid substrate (Figure 1). Because of the steric repulsion between the constrained polymer chains, polymer brushes impose osmotic pressure to the substrate $\Pi \cong k_BT/\xi^3$, which is balanced by the tension in the linkers connecting the macromolecules to the substrate ($f \cong k_BT/\xi \cong \Pi\xi^2$). This force is a small addition to bond tension within an individual chain (eq 1). However, by reconnecting the chains of a planar brush in groups of z arms, one reduces the number of linkers and, hence, increases tension per linker. In other words, multiarm grafts lead to z-fold amplification of the tension in the linker as

$$f_{linker} = zf_{arm} \quad (4)$$

which can be significantly larger than the intrinsic bond tension f_0 (eq 1). For example, a tethered star with z = 1000 arms would lead to 1000-fold amplification of the linker tension from the pN to nN scale. This new method of tension amplification is consistent with the recent reports of mechanical instability of tethered multiarm macromolecules that opt to sacrifice one covalent bond in the linker to reduce the steric repulsion between the spatially confined branches.[49−54] In this paper, we present scaling analysis of the bond tension developed in the linker between the substrate and a tethered brush-like macromolecule as a function of the number of arms, the grafting density, and the linker length. The understanding of mechanical tension in these systems is vital for many practical applications including colloids, lubricants, and antifouling coatings that rely on mechanical stability of tethered macromolecules.[55]

All theoretical predictions made in this paper use two scaling approximations. First, absolute values obtained by scaling

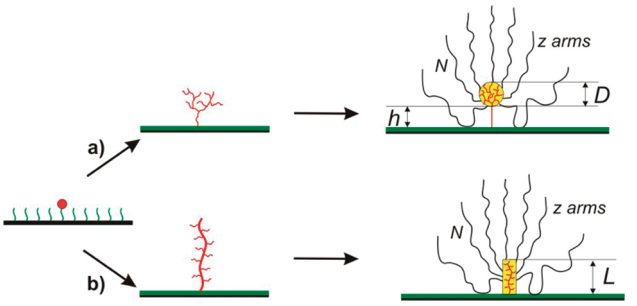

Figure 2. Two synthetic strategies for preparation of molecular stars tethered to a substrate using (a) hyperbranched and (b) "bottlebrush" macroinitiators. The hyperbranched system has a branching core of diameter D with z arms each consisting of N monomeric units. The core is connected to the substrate plane by a short spacer of length h. In the "bottlebrush" system, the arms are evenly distributed along the backbone of length L. To control the grafting density, the preparation may include dilution of the tethering sites with inactive "dummy" initiators.

analysis are accurate only up to a numerical coefficient on the order of unity. As such, numerical prefactors on the order of unity are omitted in all relations derived in this paper. Second, the paper considers the scaling regime of arm extension ($f \sim R^{\alpha}$), where R is the end-to-end distance of a chain-like polymer arm.

In this paper, we deliberately focus on the scaling regime of moderate extension of the arms ($R/R_{max} < 0.3$), since our goal is to demonstrate that multiarm grafts allow significant tension amplification ($f \gg 1$ pN) even at very low 2-D packing densities of individual arms. We will show that multiarm grafts allow tension amplification up to the nN-level enabling homolytic cleavage of covalent bonds. Furthermore, many chemical reactions, e.g. hydrolytic cleavage of siloxane bonds, may require much lower forces to be observed on conventional time scales,[52−54] which can be controlled by the mechanism of tension amplification proposed in this paper.

SYNTHETIC STRATEGIES

There are two general ways to prepare multiarm grafts.[55] In the first case, the synthesis starts with growing of a hyperbranched macroinitiator (of diameter D) at the substrate[49,56−58] followed by polymerization of linear arms at the branch-end functionalities (Figure 2a). In the second case, one first grafts a linear "bottlebrush" macroinitiator[59−61] of a contour length L followed by polymerization of linear side chains with a degree of polymerization N (Figure 2b). Preparation of branched grafts using a combination of these synthetic strategies has been reported as well.[62] Both synthetic approaches yield tethered macromolecules with multiple arms that are linked to the substrate with a single chemical bond (linker).

In the case of very long arms ($Nb \gg D$ and $Nb \gg L$), both star- and brush-like macromolecules can be approximated by a multiarm star tethered to a solid substrate with a short spacer. In both systems, the linker is under tension. However, there is one essential difference between the tethered bottle- and star-like brushes. Unlike polymer stars, where all arms sprout from a single branching center, the side chains in bottlebrushes are distributed along the backbone. As a result, the backbone tension in tethered bottlebrushes progressively increases along the backbone reaching a maximum value in the linker. Therefore, the rest of this

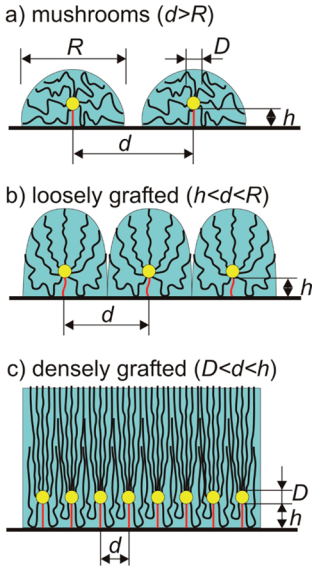

Figure 3. Three grafting regimes for multiarm star-like macromolecules tethered to a solid substrate: (a) single molecules, so-called "mushroom" regime ($d > R$), (b) loosely grafted brushes ($h < d < R$), and (c) densely grafted brushes ($D < d < h$). For all systems, the linker between the substrate and the polymer star is under tension. The loose and dense brushes offer different ways for controlling the linker tension. In loose brushes the tension depends on the linker length and does not depend on the grafting density. In dense brushes, the tension is independent of the linker length and determined by the grafting density.

paper is organized in two sections. We first calculate the linker tension in tethered stars, and then present the analysis of the tension gradient in the backbone of tethered bottlebrushes. Because of the aforementioned similarity between the systems, many equations derived for the star-like grafts will be applied to the bottlebrushes as well.

TETHERED STARS

As sketched in Figure 2, every star has a branching core of diameter D with z arms each consisting of N monomeric units of size b. The spacer consists of m monomeric units resulting in a contour length of fully stretched chain $h = mb$. For a given value of the core diameter (D), the number of arms (z) and the spacer length (h) have the upper and lower limits, respectively. The upper limit for z is given by

$$z \leq z_{\max} \cong \frac{D^2}{b^2} \tag{5}$$

which is imposed by the maximum grafting density for linear chains $\sigma \cong b^{-2}$. In this paper, we assume that the branching core has a maximum number of arms, i.e. $z = D^2/b^2$. The lower limit for the spacer length (h_{min}) is dictated by the dense packing condition of chain sections under the core, i.e. by a minimal volume $V_{min} \cong D^2 h_{min}$ that can accommodate ca. z chain sections confined between the core of diameter D and the substrate. Note that the confined chain sections are fully extended with a typical length of being on the order of D and a number of monomeric units per section $\sim D/b$. Therefore, z sections occupy a dry volume of $V_{dry} \cong z(D/b)b^3 \cong zDb^2$. From the dense packing condition ($V_{min} \cong V_{dry}$), one obtains

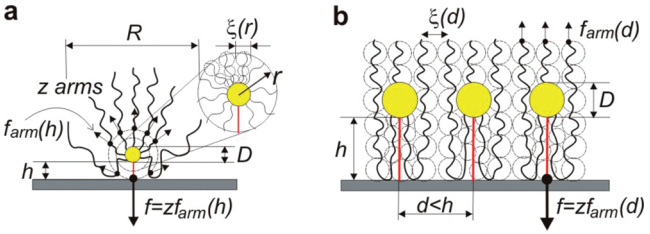

Figure 4. Star-like macromolecules tethered to a solid substrate in (a) mushroom ($d < R < h$) and (b) dense ($d < h$) brush regimes. While the chain conformation in an isolated molecule remains unperturbed at smaller distances $r \ll h$ from the branching core (inset in a), the arms get extended leading to a net repulsive force $f \cong zf_{arm}(h)$, which depends on the spacer length h. In the dense regime ($d < h$), the grafted stars behave as a planar brush with a grafting density $\sigma = 1/\xi^2 \cong z/d^2$. In this case, the tension in the individual arms is solely determined by d leading to a net repulsive force $f \cong zf_{arm}(d)$.

$h_{min} \cong zb^2/D$. For a branching core with a maximum number of arms $z \cong D^2/b^2$ (eq 5), one obtains the following relation for the minimum spacer length h

$$h \geq h_{\min} \cong D \cong \sqrt{z}b \tag{6}$$

We consider three grafting regimes depending on the average distance d between the neighboring linkers: (i) isolated macromolecules, i.e. "mushroom" regime ($d > R$, Figure 3a), where R is the size of an unperturbed star, (ii) loosely grafted brushes ($h < d < R$, Figure 3b), and (iii) dense brushes ($D < d < h$, Figure 3c). Our analysis is limited to brushes on a noninteracting substrate. On repulsive substrates, for all grafting regimes, the tension increases with respect to the noninteracting case by a correction term due to the steric repulsion from the substrate which is smaller than the main contribution to the spacer tension. On attractive substrates, the linker tension is not amplified in the mushroom regime, and it increases only at higher grafting densities.

Mushroom Regime. At low grafting densities (i.e., for large intermolecular distances $d > R$), tethered stars do not interact and can be considered as isolated macromolecules tethered to a substrate. We separately analyze the so-called wet brushes (in a solvent environment) and dry brushes (e.g., melt).

Wet Mushroom Regime. Figure 4a shows schematics of a star-like macromolecule tethered to a solid substrate with a short spacer. To visualize the process of tension generation in the linker, it is instructive to consider a free star-like macromolecule in the vicinity of a solid substrate. When the polymer star is pushed toward the substrate, it experiences a repulsive force as its linear arms explore less configurational space resulting in greater steric repulsion between the swollen linear chains. The net force f is oriented perpendicular to the substrate and increases with decreasing distance h between the branching core and the substrate. Note that conformation of the linear arms in tethered stars is almost unaffected by the substrate within a radius of $r \ll h$, and hence, do not contribute to the tension in the linker. Therefore, the linker tension predominantly results from summing up the tensions in z individual arms measured at a distance $r \cong h$, i.e., $f \cong zf_{arm}(h)$ (eq 4).

In a solvent environment, the tension in the individual arm at a radial distance r from the branching center can be estimated as

$$f_{arm}(r) \cong \frac{k_B T}{\xi(r)} \tag{7}$$

where the average distance between monomers of neighboring arms (correlation length) is given by[63]

$$\xi(r) \cong \frac{r}{\sqrt{z}} \tag{8}$$

From eqs 8 and 9, one obtains mechanical tension in the individual arm at distance r from the branching core as

$$f_{arm}(r) \cong k_B T \frac{\sqrt{z}}{r} \tag{9}$$

which gives the linker tension in a tethered star in a solvent environment as

$$f \cong z f_{arm}(h) \cong k_B T \frac{z^{3/2}}{h} \quad \text{(tethered star in the wet mushroom regime)} \tag{10}$$

The linker tension (eq 10) can be also obtained as a derivative of the interaction energy between a spherical block copolymer micelle and a substrate.[64] The distant chain sections, i.e. those located at larger distances from the branching center ($r > h$), also contribute to the tension in the linker. However, the total contribution of the distant chain sections is on the same order of magnitude as the linker tension generated by the sections located at $r \approx h$ (eq 10). Therefore, the actual tension may be higher by a factor on the order of unity, which does not affect our scaling estimates. Note also that eq 9 is equivalent to the corresponding relation for the tension in the linker of a pom-pom macromolecule with $2z$ arms.[38] Indeed, each of the pom-pom halves can be viewed as a mirror image of a tethered star, i.e., repulsion between the pom-pom branches is equivalent to the repulsion of a tethered star from a substrate.

Dry Mushroom Regime. In a nonsolvent environment, the star arms are also extended and thus under tension.[65,31] Similar to wet stars, the arm tension decreases with increasing distance from the branching center. The corresponding scaling relation can be obtained by considering a section of an individual arm of size r composed of n monomeric units. The extension force for this section can be written as

$$f_{arm} \cong k_B T \frac{r}{nb^2} \tag{11}$$

Unlike the solvent-swollen molecules, the monomer number density (number of monomers per unit volume) $c \cong b^{-3}$ does not change with the distance from the branching center and can be expressed as

$$c \cong \frac{zn}{r^3} \cong b^{-3} \tag{12}$$

From eq 12, we find $n \cong r^3/(zb^3)$ which is then substituted in eq 11 to yield the following relation for the tension in an individual arm of a dry tethered star

$$f_{arm}(r) \cong k_B T \frac{zb}{r^2} \tag{13}$$

By summing up tensions in the z arms at $r \cong h$, one obtains the tension in the linker of a tethered star in a nonsolvent environment as

$$f \cong z f_{arm}(h) \cong k_B T \frac{z^2 b}{h^2} \quad \text{(tethered star in the dry mushroom regime)} \tag{14}$$

Since $h \geq z^{1/2} b$ (eq 6), there is an upper limit for the tension as $f \leq z f_0$, with typical $f_0 \cong 1$ pN (eq 1).

Loose and Dense Brush Regimes. The tension in dense monolayers depends on the distance d between the grafting points of the z-arm stars (Figure 3b). The distance d is related to the grafting density as

$$\sigma \cong \frac{1}{d^2} \tag{15}$$

There is an upper limit for the grafting density dictated by the dense packing of z linear chains each occupying an area of b^2 (eq 5) as

$$\sigma_{\lim} \cong \frac{1}{D^2} \leq \frac{1}{zb^2} \tag{16}$$

From eq 15, the density of tethered chains can be equivalently described both by σ and d. In this paper, we will use d (the distance between the grafting sites) as a main parameter for grafting density. At $\sigma < \sigma_{lim}$, one discriminates two grafting regimes: (i) loose brush regime ($R > d > h$) and (ii) dense brush regime ($h > d > z^{1/2} b$).

Loose Brush Monolayers. In the loose brush regime, the distance between the neighboring stars is larger than the linker length ($d > h$). Similar to the mushroom regime, the major tension contribution comes from the chain sections located at a distance of $r \cong h$ from the substrate, resulting in linker tensions of $f \cong f_0 z^{3/2}/m$ (wet brush) and $f = f_0 (z/m)^2$ (dry brush) that are respectively obtained from eqs 11 and 15 with $h = mb$ and $f_0 \cong k_B T/b$ (eq 1). In other words, the tension in the linker is not significantly affected by the interaction between the neighboring macromolecules provided that they are loosely grafted to the substrate ($d > h$).

Dense Brush Monolayers. At higher grafting densities ($h > d > z^{1/2} b$, the monolayer of grafted stars is equivalent to a dense planar brush (Figure 4b) with a correlation length

$$\xi \cong \frac{d}{\sqrt{z}} \tag{17}$$

which does not depend on the linker length and is solely determined by the distance between the grafting points, i.e. grafting density. In a solvent environment, the tension per arm is obtained by substituting eq 17 into eq 7 as

$$f_{arm} \cong k_B T \frac{z^{1/2}}{d} \tag{18}$$

The sum over z arms gives the linker tension as

$$f \cong z f_{arm} \cong k_B T \frac{z^{3/2}}{d} \quad \text{(wet dense brush)} \tag{19}$$

A similar result can be obtained from the interaction energy.[64] In a nonsolvent system (dry brush, e.g., melt), the tension in individual arms is determined by dense packing of the tethered chains (eq 13) as

$$f_{arm} \cong kT \frac{zb}{d^2} \tag{20}$$

leading to the linker tension

$$f \cong z f_{arm} \cong k_B T \frac{z^2 b}{d^2} \text{ (dry dense brush)} \tag{21}$$

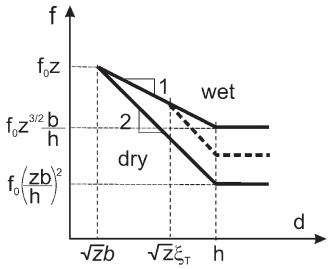

Figure 5. Tensile force in the linker between the tethered star-like brush and the substrate is presented as a function of the distance between the grafting sites d (double−logarithmic plot) for three different solvent regimes: wet (upper solid line), dry (lower solid line), and poor solvent at $\xi_T < \xi$ (dashed line). The wet regime includes good solvents ($T > \Theta$), Θ solvent ($T \cong \Theta$), and moderately poor solvents ($T < \Theta$ and $\xi_T > \xi$). For isolated molecules and loose brushes ($d > h$, $\sigma < 1/h^2$), the force does not depend on the grafting density and is determined by the length of the spacer h. At higher grafting densities, the tension increases until it reaches the maximum value of $f \cong f_0 z$ at a grafting density of $\sigma < 1/(zb^2)$. The poor solvent line (dashed) merges with the solvent line when the distance between neighboring arms becomes comparable to the thermal blob size ξ_T at $\sigma \cong 1/(z\xi_T{}^2)$.

Note that the distance between neighboring linkers is always larger than diameter of the branching core D, i.e. $d \geq z^{1/2}b$ (eq 5). Therefore, $f \leq zf_0$, where intrinsic tension $f_0 \cong k_BT/b \cong 1$ pN (eq 1).

Summary of Tension Regimes. Equations 10, 14, 19, and 21 allow estimation of the linker tension for the different grafting regimes of star-like macromolecules tethered to a solid substrate. In all cases, the tension does not depend on the degree of polymerization of the arms N as long as the star radius is larger than the spacer length ($R > h$). Grafted stars offer three independent structural parameters for tension control: (i) degree of polymerization of the spacer ($m \cong h/b$); (ii) grafting density ($\sigma \cong d^{-2}$), and the number of arms (z). Figure 5 shows how the linker tension depends on the distance between the grafting sites (i.e., grafting density). In the mushroom and loose grafting regimes ($d > h$), the tension does not depend on the grafting density and is solely controlled by the spacer length (eqs 10 and 14). On the contrary, the linker tension in the dense brush regime ($h > d > (zb)^{1/2}$) is independent of the spacer length h and increases with decreasing the intermolecular distance as $\sim d^{-1}$ in a solvent environment (eq 19) and $\sim d^{-2}$ in the dry state (eq 21). The crossover between the loose and dense brush regimes occurs at $d = h$. Upon reaching the maximum grafting density at $d \cong z^{1/2}b$ (eq 16), the linker tension attains its upper limit

$$f_{max} \cong zf_0 \qquad (22)$$

where $f_0 \cong k_BT/b$ (eq 1). For a conventional polymer with $b \cong 1$ nm and highly branched star with $z \cong 1000$, one finds $f_0 \cong 1$ pN and $f_{max} \cong 1$ nN. Note that the maximum tension (eq 22) is also attained upon shortening the spacer length to its lower limit $h \cong z^{1/2}b$ (eq 6). This can be demonstrated by substituting $h \cong z^{1/2}b$ in eq 14. In order to prepare brushes with less strained and thus more stable linkers, one should either lower the grafting density or decrease the number of arms. For example, an increase of the intermolecular distance d by a factor of 10, will drop the tension from $f \cong 1nN$ to $f \cong 0.1$ nN in solvent (eq 19) and to $f \cong 0.01$ nN in melt (eq 21). A more detailed analysis of the relevant tension values and tension amplification factors is discussed in the conclusion section.

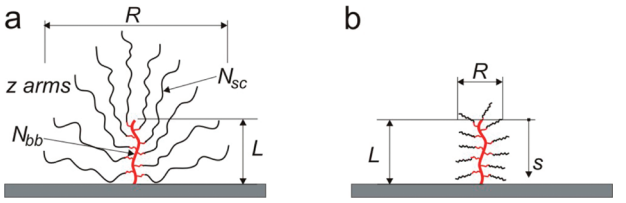

Figure 6. (a) Hairy and (b) crew-cut molecular bottlebrushes tethered to a solid substrate. The hairy brushes have star-like conformation, while the crew-cut brushes adapt a cylindrical shape.

Effect of the Solvent Quality. The effect of solvent quality on tension in the linker between a tethered star and a substrate is shown in Figure 5. In a dry state, the tension increases with grafting density as $f \sim \sigma \sim d^{-2}$ (eqs 14 and 21), which is a stronger dependence compared to $f \sim \sigma^{1/2} \sim d^{-1}$ in a solvent environment (eqs 10 and 19). At the maximum grafting density (eq 16), both systems converge to the maximum possible tension $f_{max} \cong f_0 z$ (eq 22). Note that the maximum tension depends neither on the solvent quality nor on the grafting density, i.e. the upper tension limit is the same for dry, wet, single molecules, loose, and dense brushes.

In the dense brush regime ($z^{1/2}b < d < h$), the difference in tension between the dry and wet brushes increases with distance d between the grafting sites. At a transition from the densely to loosely grafted brushes at $d \cong h$, the "wet-to-dry" force ratio can be calculated from the ratio of eqs 10 and 14 as $f_{wet}/f_{dry} \cong h/(z^{1/2}b) \cong h/D$, where $D \cong z^{1/2}b$ is the diameter of the branching core (eq 5). In other words, the linker tension in a solvent environment can be larger than the tension in the dry state by a factor of h/D (note that $h \geq D$ (eq 6)). It is important to emphasize that the solvent quality has an effect on the tension value only at $T < \Theta$ (poor solvent).[38] Under good solvent conditions ($T > \Theta$), in a Θ solvent ($T \cong \Theta$), and even in a range of poor solvents ($T < \Theta$), the linker tension virtually does not depend on solvent quality and follows eqs 10 and 19 (upper solid line in Figure 6). The effect of solvent quality at $T < \Theta$ becomes noticeable when the distance between the star arms becomes larger than the size of the thermal blob $\xi_T \cong b(\Theta - T)/T$ (dashed line in Figure 5). In this regime ($\xi > \xi_T$), tethered stars can be considered as a melt of thermal blobs. As such, the linker tension in this poor solvent regime can be calculated by replacing the monomer concentration $c \cong b^{-3}$ in eq 12 with $c \cong g_T/\xi_T{}^3 \cong 1/(\xi_T b^2)$, where g_T, the number of monomeric units within the thermal blob, is related to the blob size ξ_T as $\xi_T{}^2 = g_T b^2$.[40] This gives the following relations for the linker tension in tethered stars in a poor solvent environment at $\xi_T < \xi$:

$$f \cong k_B T z^2 \frac{\xi_T}{h^2} \quad \text{mushroom in a poor solvent } (d > h) \qquad (23)$$

$$f \cong k_B T z^2 \frac{\xi_T}{d^2} \quad \text{dense brush in a poor solvent } (\sqrt{z}\xi_T < d < h) \qquad (24)$$

TETHERED "BOTTLEBRUSHES"

Molecular bottlebrushes tethered to a substrate (Figure 2b) represent another system that allows amplification of bond tension from the pN to nN range. There are two representative

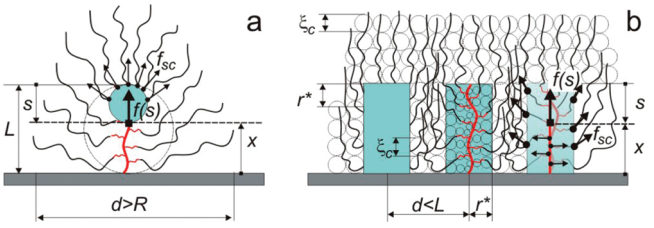

Figure 7. Two grafting regimes of molecular bottlebrushes tethered to a solid substrate: (a) isolated macromolecule (mushroom, $d > R$) and (b) densely grafted bottlebrushes ($L > d > z^{1/2}b$). The schematics of the mushroom regime (a) is also relevant to the loosely grafted macromolecules ($R > d > L$), since side-chain conformation remains unperturbed by the neighboring brushes within the dashed circle of diameter L in part a.

cases: hairy brushes ($R \gg L$, Figure 6a) and crew-cut brushes ($R \ll L$, Figure 6b), where R is the lateral size of a tethered molecule determined by its side chains and L is the backbone length. In this paper, we focus on hairy brushes that demonstrate progressive increase of tension along the backbone. In crew-cut bottlebrushes, the tension increase is observed only at the free end of their backbones, similarly to the tension variation in untethered brushes.[37]

Figure 6a shows dimensions of a tethered bottlebrush with z side chains. The degrees of polymerization (DP) of the backbone and side chains are N_{bb}, and N_{sc}, respectively. The contour lengths of the brush backbone is given by

$$L = N_{bb}b = zb \tag{25}$$

Note that $N_{bb} = z$ as we assume that every monomeric unit of the backbone has one side chain. Similar to grafted stars, one considers three regimes that corresponds to the so-called mushroom ($d > R$), loosely tethered "bottlebrushes" ($R > d > L$), and densely tethered "bottlebrushes" ($L > d > z^{1/2}b$). We start with the mushroom regime (isolated molecules), which is also relevant to loosely tethered macromolecules.

Mushroom Regime. If the distance between the neighboring bottlebrushes is larger than the contour length of the brush backbone ($d > L$), the backbone tension is largely controlled by steric repulsion of the side chains within an individual molecule. At a distance s from the backbone free end (Figure 7a), the backbone tension $f(s)$ is obtained as a sum of tensile forces f_{sc} from the individual side chains attached to the backbone within distance s from the free end. At equilibrium, when all forces are balanced, this brush section may be considered as a star-like macromolecule, which is tethered to an imaginary substrate located at a distance $x = L - s$ from the real substrate (dashed line in Figure 7a) . In this case, the backbone tension at distance s from the free end can be directly obtained from eqs 10 and 14 as a tension in the spacer between the imaginary substrate and a star-like macromolecule with $z = s/b$ arms. Using $h = s$ for the spacer length, eqs 10 and 14 give the corresponding scaling relations for the tension variation along the backbone of a tethered bottlebrush in a solvent environment and dry state:

$$f(s) \cong f_0\sqrt{\frac{s}{b}} \quad \text{wet bottlebrush} \tag{26}$$

$$f \cong f_0 \quad \text{dry bottlebrush} \tag{27}$$

where intrinsic tension $f_0 \cong 1$ pN is given by eq 1. Note that in the dry state (eq 27), the backbone tension does not depend on the

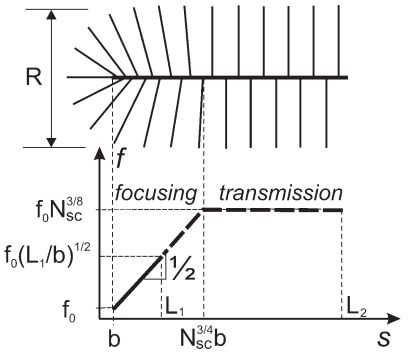

Figure 8. The log−log plot shows the development of backbone tension within a tethered bottlebrush in the mushroom regime as a function of distance s from the free end of the backbone. The plot combines a hairy-brush system ($L_1 < R$, solid line) and a crew-cut system ($L_2 > R$, dashed line), where $R \cong N_{sc}^{3/4}b$ is the lateral dimension of the bottlebrush in a good solvent. In a hairy brush, the tension increases as $f \sim \sqrt{s}$ (eq 26). Once the backbone length becomes longer than R (crew-cut), the tension levels off at $f \cong f_0N_{sc}^{3/8}$.[37] In a crew-cut brush, the ranges $L < R$ and $L > R$ are called as focusing and transmission zones, respectively.

distance along the backbone and adopts its maximum value on the order of $f_0 \cong 1$ pN. This is consistent with the behavior of free (nontethered) brushes in a melt state.[37] Unlike dry brushes, the backbone tension in a wet brush (eq 26) increases from $f \cong f_0$ at $s = b$ (first bond at the free end of the backbone) to its maximum value in the linker at $s = L \cong zb$

$$f_{linker} \cong f_0\sqrt{z} \quad \text{(bottlebrush in the wet mushroom regime)} \tag{28}$$

Note that the upper limit of the linker tension in a tethered bottlebrush is by a factor of $\sqrt{z}$ smaller than the maximum tension in a tethered star with the same number of arms z (eq 22). This reduction is due to the distribution of the side chains (and hence, their tensions) along the backbone of length $L \cong zb \sim z$ (unlike tethered stars with z arms sprouting from a spherical core of size $D \cong z^{1/2}b \sim \sqrt{z}$).

Another important conclusion from eq 26 is that the backbone tension in hairy bottlebrushes ($L < R$) does not depend on the degree of polymerization of side chains N_{sc} (see Figure 6a). This behavior is different from that of crew-cut brushes ($L \gg R$) that exhibit a constant tension of $f \cong f_0N_{sc}^{3/8}$ along the central section of the backbone, the so-called transmission zone.[37] Figure 8 demonstrates the development of the backbone tension as a function of s for both hairy ($L_1 < R$) and crew-cut ($L_2 > R$) wet bottlebrushes. In the hairy system (Figure 6a), the tension follows eq 26 (solid line). In a crew-cut brush (Figure 6b), the tension first increases and then levels off at a distance $s = R$, where $R \cong N_{sc}^{3/4}b$ is the lateral size of the bottlebrush. By substituting $s \cong N_{sc}^{3/4}b$ in eq 26, we obtain the plateau value $f \cong f_0N_{sc}^{3/8}$, which exactly corresponds to the backbone tension of a free bottlebrush molecule in a good solvent.[37] In the previous paper,[37] the end-cup of the bottlebrush ($s < R$) is called the focusing zone, i.e. the zone of tension amplification, while the central section of the brush $R < s < L$ is called the transmission zone, which transmits the tension from the brush end to the substrate.[37]

Loosely and Densely Tethered Molecular Bottlebrushes. At intermolecular distances smaller than the lateral dimension of a bottlebrush ($d < R$), the conformations of the side chains are

dx.doi.org/10.1021/ma200328h |Macromolecules 2011, 44, 4520–4529

perturbed due to the overlap with the neighboring bottlebrushes (Figure 7b). Similar to tethered stars (Figure 4), one discriminates two grafting regimes for bottlebrush monolayers, i.e., loosely and densely grafted macromolecules.

Loose Bottlebrush Monolayers. The loose-brush regime is observed when the distance between the neighboring bottlebrushes is smaller than their lateral size R, yet larger than the contour length L of its backbone ($L < d < R$). In this regime, the conformation of the side chains in the brush core is largely unperturbed within a radius $r < L$ from the backbone. Similar to our analysis of the mushroom regime (Figure 7a), a tethered bottlebrush may be considered as a star-like macromolecule at any distance s ($0 < s < L$) from the backbone end, which allows using eqs 26 and 27 for calculation of the backbone tension in wet and dry brushes, respectively.

Dense Bottlebrush Monolayers. Here, we first consider wet brushes, i.e. tethered bottlebrushes in the presence of solvent. In the dense brush regime ($z^{1/2}b < d < L$), the side chains of the neighboring brushes partially overlap and change their conformation (hence, tension). In this regime, every brush molecule can be considered as a core−shell cylinder with a total radius of $r = d/2$ and a core radius of $r = r^*$ (Figure 7b). Within the core ($0 < r < r^*$), the extended conformation of the side chains remains unperturbed by the neighboring bottlebrushes. In the overlap region ($r^* < r < d/2$), the excluded volume repulsion between the side chains is screened on length scales larger than the correlation length ξ_c. Therefore, the space in the overlap region is filled by a melt of the so-called correlation blobs of size ξ_c. The chains of correlation blobs are extended due to repulsion between neighboring brushes.

The variation of tension along the backbone depends on distance s from the free end of the backbone. Close to the backbone end ($s < r^*$), the backbone does not feel the presence of the neighboring bottlebrushes and behaves similar to the isolated macromolecules in the mushroom regime. Therefore, the backbone tension in the range $s < r^*$ is given by eq 26. On larger length scales ($s > r^*$), the backbone tension is affected by the interaction with the neighbors. Akin to the tug-of-war game, the backbone tension at a distance x from the substrate is a sum of individual tensions $f_{sc}(x)$ from the side-chains located above the x-plane. This can written as an integral

$$f(s) \cong \sum_{i=g}^{z} f_{sc}^{i} \cong \int_{L-s}^{L} f_{sc}(x') \frac{dx'}{b} \tag{29}$$

where $g \cong x/b$ is the number of branching points in the backbone section located below the x-plane ($0 \le x \le L - s$) (Figure 7b). In the overlap region, every side-chain can be considered as a chain of correlation blobs (effective monomers) extended perpendicular to the substrate with a tension force

$$f_{sc}(x) \cong k_B T \frac{x}{m\xi_c^{\,2}} \tag{30}$$

where x is the size of a chain section composed of m correlation blobs of size ξ_c. The blob size is obtained from the area-filling condition, i.e. each side chain occupies an area $\xi_c^{\,2} \cong d^2/z$. This gives the size of the correlation blob as

$$\xi_c \cong \frac{d}{\sqrt{z}} \tag{31}$$

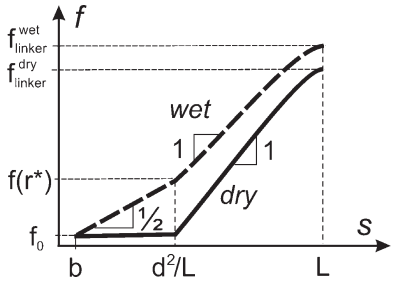

Figure 9. Tension in the backbone of densely tethered ($d < L$) bottlebrushes increases with the distance from the free end of the backbone (log−log plot). At short distances ($s < r^*$), the end-cup of a tethered bottlebrush does not feel the pressure of the neighboring brushes and behaves as a free (nontethered) bottlebrush. In this regime, the tension variation in wet and dry brushes is given by $f \sim \sqrt{s}$ (eq 26, dashed line) and $f \cong f_0$ (eq 27, solid line), respectively. At a distance of $s \cong r^* \cong d^2/L$, the brush becomes perturbed by the neighboring brushes and switches its tension variation to $f \sim s$ (eq 36 and eq 42 for wet and dry brushes, respectively). The crossover point between the two regimes is defined by eqs 37 and 38. The linker tension ($s = L$) is given by eqs 39 and 43 for wet and dry brushes, respectively.

The number of correlation blobs per side-chain section confined within a volume of $v \cong xd^2 \cong gbd^2$ is calculated from the space-filling condition as

$$m \cong \frac{v}{g\xi_c^{\,3}} = \frac{bd^2}{\xi_c^{\,3}} \tag{32}$$

by considering volume v filled by a melt of mg densely packed correlation blobs, i.e. by g chain sections of volume $m\xi_c^{\,3}$ each. Using eq 31 for the blob size, one rewrites eq 32 as

$$m \cong bz^{3/2}/d \tag{33}$$

Note that m (number of blobs in a chain section of size x) does not depend on the section size x because both the volume v and the number of chains in that volume are proportional to x. By substituting eqs 31 and 33 in eq 30, one obtains that the tension in a side chain increases linearly with its position (x) along the backbone

$$f_{sc}(x) \cong \frac{f_0}{d\sqrt{z}} x \tag{34}$$

where f_0 is the intrinsic bond tension (eq 1). The side-chain tensions are integrated (eq 29) to yield the backbone tension at distance s from the free end of the backbone

$$f(s) \cong f_0 \frac{s(2L - s)}{2bd\sqrt{z}} \tag{35}$$

At large distances from the backbone end ($s \cong L$), i.e., close to the substrate, the backbone tension (eq 35) exhibits parabolic dependence on s. However, at smaller distances ($s \ll L$), the tension depends on the distance nearly linearly, i.e. $f(s) \sim s$. By substituting the backbone length $L \cong bz$ (eq 25) in eq 35 one obtains the variation of the backbone tension in terms of the structural parameters of the system (b, z, d)

$$f(s) \cong f_0 \frac{\sqrt{z}}{d} s \quad (r^* < s \ll L) \tag{36}$$

As discussed above, the end-caps of densely tethered bottlebrushes ($s < r^*$) behave as loosely tethered brushes with a

Table 1. Relations and Values for Bond Tension in Tethered Macromolecules

system/property	scaling relation	value
1. Planar Brushes		
$T = 298$ K, $b \cong 1$ nm, $\sigma_{max} \cong 1.4$ nm^{-2} (eq 4)		
linker tension in a single chain tethered to a substrate	$f_0 \cong \frac{k_B T}{b}$ (1)	4 pN
extra tension in a dense brush ($\sigma \cong 0.4$ nm^{-2})[41]	$f \cong \frac{k_B T}{b} \cong k_B T\sqrt{\sigma}$	2.5 pN
2. Tethered Stars ($m \geq \sqrt{z}$, e.g. $m = 100$, $z = 900$, and $b = 1$ nm)		
2.1 Mushroom and Loose Grafting Regimes ($d > h \cong mb \cong 100$ nm)		
wet brush (good, Θ, and moderately poor solvent)	$f \cong f_0 \frac{z^{3/2}}{m}$ (10)	1 nN
dry brush (melt)	$f \cong f_0 \left(\frac{z}{m}\right)^2$ (14)	300 pN
2.2 Dense Grafting Regime ($z^{1/2}b < d < h$, e.g., $d \cong 50$ nm)		
wet brush (good, Θ, and moderately poor solvent)	$f \cong f_0 z^{3/2} \frac{b}{d}$ (19)	2 nN
dry brush (melt)	$f \cong f_0 z^2 \left(\frac{b}{d}\right)^2$ (21)	1 nN
3. Tethered Bottlebrushes ($L \leq R$, $d \geq z^{1/2}b$, $z \cong 900$, $b \cong 1$ nm)		
3.1 Mushroom and Loose Grafting Regimes ($d > L \cong bz \cong 900$ nm)		
wet brush (good, Θ, and moderately poor solvent)	$f_{linker} \cong f_0\sqrt{z}$ (28)	100 pN
dry brush (melt)	$f \cong f_0$ (27)	4 pN
3.2 Dense Grafting Regime ($z^{1/2}b < d < L$, e.g., $d \cong 50$ nm)		
wet brush (good, Θ, and moderately poor solvent)	$f_{linker} \cong f_0 z^{3/2} \frac{b}{d}$ (39)	2 nN
dry brush (melt)	$f_{linker} \cong f_0 z^2 \frac{b^2}{d^2}$ (43)	1 nN

backbone tension given by eq 26, i.e., $f(s) \sim \sqrt{s}$. Both expressions for tension (eqs 26 and 36) should match at $s = r^*$, where r^* is given by

$$r^* \cong \frac{d^2}{L} \tag{37}$$

The length scale given by eq 37 can be regarded as a crossover from the intramolecular to intermolecular brush systems. Since $d \ll L$ (dense brush regime), the crossover occurs at a relatively small distance from the backbone end ($r^* \ll L$). One can calculate the backbone tension at the crossover point ($s = r^*$) as

$$f(r^*) \cong f_0 \frac{d}{b\sqrt{z}} \tag{38}$$

eqs 26 and 36 have been used to plot the variation of the backbone tension as a function of the distance s from the free end of the backbone (Figure 9).

The tension in the linker can be obtained by substituting $s = L \cong bz$ in eq 36 as

$$f_{linker} \cong f(L) \cong f_0 z^{3/2} \frac{b}{d} \quad \text{(wet densely tethered bottlebrushes)} \tag{39}$$

It is instructive to calculate the linker tension for the two grafting density limits of the dense brush regime. At the crossover from the loose to dense brush regime ($d = L \cong bz$), the linker tension is given by

$$f_{linker} \cong f_0\sqrt{z} \quad (d \cong L) \tag{40}$$

which coincides with the linker tension in the mushroom and loosely grafted regimes (eq 28). When the grafting density approaches its physical limit $d \cong b\sqrt{z}$ (eq 16) one obtains

$$f_{linker} \cong f_0 \frac{L}{b} \cong z f_0 \quad (d \cong b\sqrt{z}) \tag{41}$$

which is equal to the maximum linker tension in densely grafted stars with the same number of arms (eq 22).

Densely Tethered Bottlebrushes in a Dry State. In dry brushes, the correlation blob is on the order of monomeric size. Therefore, to calculate the variation of the backbone tension in dry brushes, one should substitute $\xi_c \cong b$ in eqs 31 and 32, and then follow the same protocol used for the derivation of the backbone tension in the wet regime (eq 36). This gives the following relations for the variation of the backbone tension as a function of

dx.doi.org/10.1021/ma200328h |*Macromolecules* 2011, 44, 4520–4529

the distance from the backbone end:

$$f(s) \cong f_0 \frac{bz}{d^2} s \tag{42}$$

At the free end of the backbone ($s < r^*$), the backbone tension is not affected by the neighboring brushes. Within this so-called focusing zone (Figure 8), the tension is determined by eq 27; i.e., it depends neither on grafting density nor the distance along the backbone. The onset of the tension increase (eq 42) occurs in the crossover region at $s = r^* \cong d^2/L$, which is calculated by equating 27 and 42 and is identical to eq 37. In other words, in the dense grafting regime, the effect of the neighboring brushes becomes noticeable on the same length scale for wet and dry bottlebrushes.

Akin to the wet brushes (eq 39), the tension in the linker is obtained by substituting $s = L \cong bz$ in eq 42 as

$$f_{linker} \cong f_0 z^2 \left(\frac{b}{d}\right)^2 \quad \text{(dry densely tethered bottlebrushes)} \tag{43}$$

At the transition from the loose to dense grafting regime ($d \cong L$), the linker tension in a dry bottlebrush is equal to $f_{linker} \cong f_0$ (eq 27), while at the upper limit for the grafting density $d \cong b\sqrt{z}$ (eq 16), the linker tension approaches the maximum value given by $f_{linker} \cong f_0 z$ (eq 22). From eqs 39 and 43, one concludes that the linker tension in wet brushes is larger than the tension in dry brushes by a factor of

$$\frac{f_{\text{linker}}^{\text{wet}}}{f_{\text{linker}}^{\text{dry}}} \cong \frac{d}{b\sqrt{z}} \tag{44}$$

Note that the interbrush distance d cannot be smaller than $\sigma_{lim}^{-1/2} \cong b\sqrt{z}$ (eq 16).

CONCLUSIONS

We have shown that tethering multiarm macromolecules to a solid substrate leads to significant amplification of tension in the linker. The derived equations provide scaling relations between the linker tension and the controlled synthetic parameters, including the number of arms (z), the linker length (h), and the grafting density ($\sigma \cong 1/d^2$). In the case of tethered bottlebrushes, one may also introduce an additional parameter $p \cong N_{bb}/z \geq 1$, i.e. a number of the backbone Kuhn monomeric units per side chain, which corresponds to the intramolecular linear grafting density $1/(pb)$.[37] A decrease in the grafting density ($p > 1$) would lower the backbone tension. In conventional systems, $p \cong 1$. Table 1 summarizes useful relations that can be applied for estimating the linker tension in two different molecular architectures, i.e. tethered polymer stars and tethered bottlebrushes, in both solvent and nonsolvent environments. To demonstrate the amplification effect of the branched architecture, the table includes the corresponding scaling relations for conventional planar brushes. The table shows that depending on the linker length and the grafting density, one can achieve z-fold amplification of the linker tension from the pN to nN scale, i.e., from $f_0 \cong 1$ pN (eq 1) to $zf_0 \cong 1nN$ (eq 22). Increasing the linker length $h \cong mb$ and the intermolecular distance d above their lower limits $h_{min} \cong d_{min} \cong z^{1/2}b$ (eqs 6 and 16), results in tension decrease as $1/m$ and $1/d$ in wet brushes and as $1/m^2$ and $1/d^2$ in dry brushes, respectively. Using equations in Table 1, one can calculate the d- and z-amplification factors, i.e. $\partial f/\partial d$ and $\partial f/\partial z$ derivatives, to quantify the effect the grafting density and the number of arms on the tension value. For example, in wet densely tethered stars, the d-amplification factor for the linker tension is given by

$$\frac{\partial f}{\partial d} \cong -f_0 z^{3/2} \frac{b}{d^2}$$

For a given set of parameters ($b = 1$ nm, $z = 900$, $d = 100$ nm), one obtains $\partial f/\partial d \cong -40$ pN/nm, i.e the linker tension increases by 40 pN upon decreasing the distance between tethered macromolecules by 1 nm. Correspondingly, one can calculate the z-amplification factor for the linker tension in wet densely tethered stars as

$$\frac{\partial f}{\partial z} \cong f_0 \sqrt{z} \frac{b}{c}$$

For the same set of molecular parameters ($b = 1$ nm, $z = 900$, $d = 100$ nm), one obtains $\partial f/\partial z \cong 3$ pN/arm; i.e., the linker tension increases by 3 pN upon adding one extra arm. Using eq 3, these amplification factors can be translated to acceleration of the bond-scission process. For example, 10-fold enhancement of the scission rate occurs when the bond tension increases by $\Delta f \cong 250$ pN. This is equivalent to either a decrease of the intermolecular distance by $\Delta d \cong 6$ nm or increase of the number of arms by $\Delta z \cong 70$. These estimates are vital for forecasting the mechanical stability of tethered polymer brushes.

AUTHOR INFORMATION

Corresponding Author

*E-mail: sergei@email.unc.edu.

ACKNOWLEDGMENT

We gratefully acknowledge funding from the National Science Foundation (DMR 0906985, CBET-0609087, CHE-0911588, and DMR-0907515) and the National Institutes of Health (R01-HL077546-03A2). We are grateful to A. Grosberg for a very illuminating suggestions.

REFERENCES

(1) Li, S.; Guan, J.-L.; Chien, S. *Annu. Rev. Biomed. Eng.* **2005**, *7*, 105–150.
(2) Ingber, D. E. *FASEB* **2006**, *20*, 811–827.
(3) Piazzesi, G.; Reconditi, M.; Linari, M.; Lucii, L.; Sun, Y. B.; Narayanan, T.; Boesecke, P.; Lombardi, V.; Irving, M. *Nature* **2002**, *415*, 659–662.
(4) Vale, R. D.; Milligan, R. A. *Science* **2000**, *288*, 88–95.
(5) Carter, N. J.; Cross, R. A. *Nature* **2005**, *435*, 308–312.
(6) Evans, E. A.; Calderwood, D. A. *Science* **2007**, *316*, 1148–1153.
(7) Discher, D. E.; Janmey, P.; Wang, Y.-l. *Science* **2005**, *310*, 1139–1143.
(8) Wong, J. Y.; Velasco, A.; Rajagopalan, P.; Pham, Q. *Langmuir* **2003**, *19*, 1908–1913.
(9) Lo, C.-M.; Wang, H.-B.; Dembo, M.; Wang, Y-l. *Biophys. J.* **2000**, *79*, 144–152.
(10) Mitchison, T. J.; Cramer, L. P. *Cell* **1996**, *84*, 371–379.
(11) Legant, W. R.; Miller, J. S.; Blakley, B. L.; Cohen, D. M.; Genin, G. M.; Chen, C. S. *Nature Methods* **2010**, *7*, 969–972.
(12) Beyer, M. K.; Clausen-Schaumann, H. *Chem. Rev.* **2005**, *105*, 2921–2948.
(13) Caruso, M. M.; Davis, D. A.; Shen, Q.; Odom, S. A.; Sottos, N. R.; White, S. R.; Moore, J. S. *Chem. Rev.* **2009**, *109*, 5755–5776.

(14) Odell, J. A.; Keller, A. *J. Polym. Sci., Part B* **1986**, *24*, 1889–1916.
(15) Bensimon, D. *Structure (London)* **1996**, *4*, 885–887.
(16) Evans, E. *Annu. Rev. Biophys. Biomol. Struct.* **2001**, *30*, 105–128.
(17) Hickenboth, C. R.; Moore, J. S.; White, S. R.; Scottos, N. R.; Baudry, J.; Wilson, S. R. *Nature* **2007**, *446*, 423–427.
(18) Lenhardt, J. M.; Craig, S. L. *Nature Nanotechnol.* **2009**, *4*, 284–285.
(19) Wiita, A. P.; Ainavarapu, R. K.; Huang, H. H.; Fernandez, J. M. *Proc. Natl. Acad. Sci. U. S. A.* **2006**, *103*, 7222–7226.
(20) Ribas-Arino, J.; Shiga, M.; Marx, D. *Angew. Chem., Int. Ed.* **2009**, *48*, 4190–4193.
(21) Yang, Q. Z.; Huang, Z.; Kucharski, T. J.; Khvostichenko, D.; Chen, J.; Boulatov, R. *Nature Nanotechnol.* **2009**, *4*, 302–306.
(22) Rohrig, U. F.; Troppmann, U.; Frank, I. *Chem. Phys.* **2003**, *289*, 381–388.
(23) Davis, D. A.; Hamilton, A.; Yang, J. L.; Cremar, L. D.; Van Gough, D.; Potisek, S. L.; Ong, M. T.; Braun, P. V.; Martinez, T. J.; White, S. R.; Moore, J. S.; Sottos, N. R. *Nature* **2009**, *459*, 68–72.
(24) Todres, Z. V. *J. Chem. Res.* **2004**, *2*, 89–93.
(25) Tipikin, D. S. *Russ. J. Phys. Chem.* **2001**, *75*, 1876–1879.
(26) Parks, J. J.; Champagne, A. R.; Costi, T. A.; Shum, W. W.; Pasupathy, A. N.; Neuscamman, E.; Flores-Torres, S.; Cornaglia, P. S.; Aligia, A. A.; Balseiro, C. A.; Chan, G. K.-L.; Abruña, H. D.; Ralph, D. C. *Science* **2010**, *328*, 1370–1373.
(27) Bell, G. I. *Science* **1978**, *200*, 618–626.
(28) Farkas, Z.; Derenyi, I.; Vicsek, T. *J. Phys.: Condens. Matter* **2003**, *15*, S1767–S1777.
(29) DeGennes, P. G. *Macromolecules* **1980**, *13*, 1069–1076.
(30) Alexander, S. *J. Phys. (Paris)* **1977**, *38*, 983–988.
(31) Semenov, A. N. *Sov. Phys. JETP* **1985**, *61*, 733–739.
(32) Birshtein, T. M.; Borisov, O. V.; Zhulina, E. B.; Khokhlov, A. R.; Yurasova, T. A. *Polym. Sci. USSR* **1987**, *29*, 1169–1178.
(33) Grest, G. S. *Macromolecules* **1993**, *26*, 3108–3116.
(34) Milner, S. T. *Macromolecules* **1988**, *21*, 2610–2616.
(35) Chen, W. Y. *Phys. Rev. Lett.* **2004**, *93*, 028301/1–4.
(36) Sheiko, S. S.; Sun, F. C.; Randal, A.; Shirvaniants, D.; Matyjaszewski, K.; Rubinstein, M. *Nature* **2006**, *440*, 191–194.
(37) Panyukov, S. V.; Zhulina, E. B.; Sheiko, S. S.; Randall, G.; Brock, J.; Rubinstein, M. *J. Phys. Chem.* **2009**, *113*, 3750–3768.
(38) Panyukov, S. V.; Sheiko, S. S.; Rubinstein, M. *Phys. Rev . Lett.* **2009**, *102*, 148301/1–4.
(39) de Gennes, P.-G. *Scaling Concepts in Polymer Physics*; Cornell University Press: Ithaca, NY, 1979).
(40) Rubinstein, M.; Colby, R. H. *Polymer Physics*; Oxford Press: New York, 2006.
(41) Yamamoto, S.; Ejaz, M.; Tsujii, Y.; Fukuda, T. *Macromolecules* **2000**, *33*, 5602–5608.
(42) Kauzmann, W. J.; Eyring, H. *J. Am. Chem. Soc.* **1940**, *62*, 3113–3120.
(43) Zhurkov, S. N. *Int. J. Fract. Mech.* **1965**, *1*, 311–319.
(44) Bell, G. I. *Science* **1978**, *200*, 618–624.
(45) Dobrynin, A. V.; Carrillo, J.-M. Y.; Rubinstein, M. *Macromolecules* **2010**, *43*, 9181–9190.
(46) Lebedeva, N. V.; Sun, F. C.; Lee, H.-I.; Matyjaszewski, K.; Sheiko, S. S. *J. Am. Chem. Soc.* **2008**, *130*, 4228–4229.
(47) Park, I.; Nese, A.; Matyjaszewski, K.; Sheiko, S. S. *Macromolecules* **2009**, *42*, 1805–1807.
(48) Park, I.; Shirvanyants, D.; Nese, A.; Matyjaszewski, K.; Rubinstein, M.; Sheiko, S. S. *J. Am. Chem. Soc.* **2010**, *132*, 12487–12491.
(49) Deng, Y.; Zhu, X.-Y. *J. Am. Chem. Soc.* **2007**, *129*, 7557–7561.
(50) Branch, D. W.; Wheeler, B. C.; Brewer, G. J.; Leckband, D. E. *Biomaterials* **2001**, *22*, 1035–1047.
(51) Sharma, S.; Johnson, R. W.; Desai, T. A.; Dorothy, M. D. *Langmuir* **2004**, *20*, 348–356.
(52) Tugulu, S.; Klok, H. A. *Biomacromolecules* **2008**, *9*, 906–912.
(53) Paripovic, D.; Klok, H.-A. *Macromol. Chem. Phys.* **2011**, *212*, 950–958.
(54) Schmidt, S. W.; Kersch, A.; Beyer, M. C.; Clausen-Schaumann, H. *Phys. Chem. Chem. Phys.* **2011**, *13*, 5994–5999.
(55) Barbey, R.; Lavanant, L.; Paripovic, D.; Schuwer, N.; Sugnaux, C.; Tugulu, S.; Klok, H.-K. *Chem. Rev.* **2009**, *109*, 5437–5527.
(56) Mori, H.; Müller, A. H. E. *Top. Curr. Chem.* **2003**, *228*, 1–37.
(57) Liu, P.; Wang, T. M. *Polym. Eng. Sci.* **2007**, *47*, 1296–1301.
(58) Xu, F. J.; Yuan, Z. L.; Kang, E. T.; Neoh, K. G. *Langmuir* **2004**, *20*, 8200.
(59) Lee, H. J.; Nakayama, Y.; Matsuda, T. *Macromolecules* **1999**, *32*, 6989–6995.
(60) Xu, F. J.; Zhong, S. P.; Yung, L. Y. L.; Tong, Y. W.; Kang, E.-T.; Neoh, K. G. *Biomaterials* **2006**, *27*, 1236–1245.
(61) Zhai, G. Q.; Cao, Y.; Gao, J. *J. Appl. Polym. Sci.* **2006**, *102*, 2590–2599.
(62) Nakayama, Y.; Sudo, M.; Uchida, K.; Matsuda, T. *Langmuir* **2002**, *18*, 2601–2606.
(63) Daoud, M.; Cotton, J. P. *J. Phys. (Paris)* **1982**, *43*, 531–538.
(64) Johner, A.; Joanny, J. F. *Macromolecules* **1990**, *23*, 5299–5311.
(65) Birshtein, T. M.; Zhulina, E. B. *Polymer* **1989**, *30*, 170–178.